III. R & D RELATED TO A FUTURE RARE ISOTOPE ACCELERATOR FACILITY

A. INTRODUCTION

Intense efforts over the past few years, supported in part by Argonne Laboratory Directed Research and Development (LDRD) funds, have led to an exciting concept for an advanced facility for beams of exotic short-lived nuclei of the ISOL (Isotope Separation On Line) type. Such a facility is based on an intense driver beam that produces short-lived nuclear species which are stopped, the desired isotope is selected, and accelerated to the appropriate energy in a second accelerator.

The recent Argonne work involves a number of technical innovations. Most importantly, it includes a novel approach that avoids the most serious drawbacks of an ISOL facility for a broad range of beams: delay between the production of the short-lived isotopes and their acceleration and the underlying sensitivity to the chemistry of extracted species. A scheme has been developed which provides for shorter delay times and insensitivity to the chemical properties. It is based on intense heavy-ion beams from the production linac, the use of the projectile fragmentation mechanism, and subsequent extraction of the desired fragment from a high-pressure helium-gas stopper cell.

The overall Argonne concept aims squarely at providing the intense beams of short-lived nuclei needed to carry out the research described in the community White Paper (1997) on the Science Opportunities with an ISOL Facility. Our initial plans, described in the 1995 Argonne Working Paper (***ANL Yellow Book***), have found widespread attention. The concept of using a high-power primary linac for light and heavy ions, including the generation of fast neutrons from a deuteron beam for a two-step production scheme, has triggered broad international interest.

The current concept builds and expands on these initial ideas, with several new developments: *i)* ***a super-conducting cw production linac***, providing intense beams of light and light heavy-ions with beam power of up to 400 kW, and heavy ions up to uranium at 100 kW; *ii)* ***2- step targets*** to handle beam powers in excess of 100 kW; *iii)* utilization of a ***range of reaction mechanisms*** to optimize yields of radioactive ions

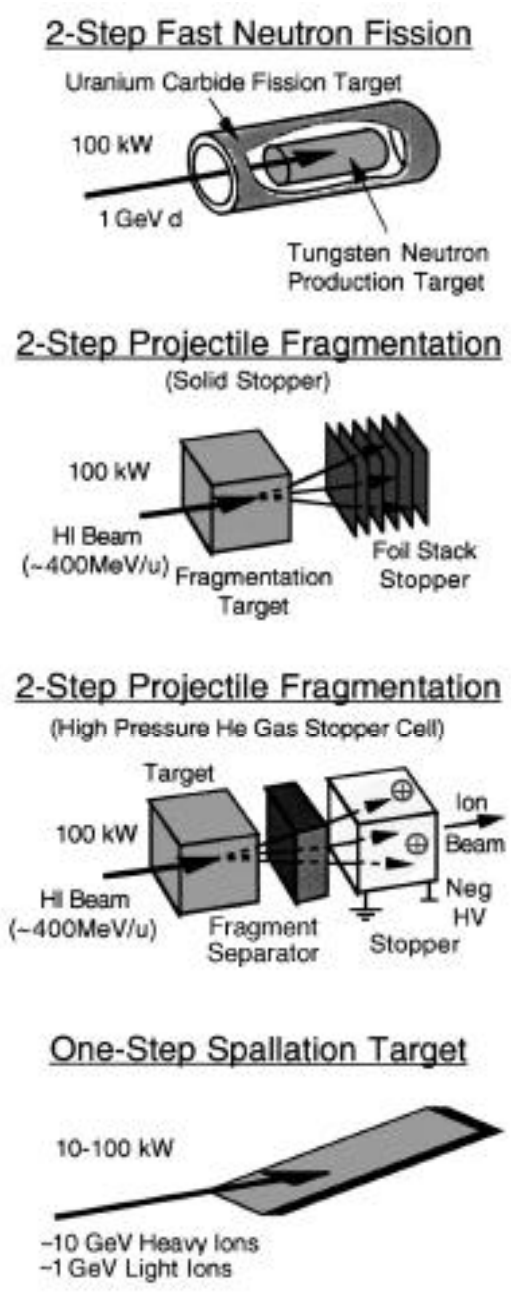

Fig. III-1 Production target concepts RIA.

and to match the high-power target concepts; *iv)* development of a cw injector into ATLAS, with a new ***RFQ accelerator for 1^+ ions*** and non-equilibrium low-velocity stripping; and *v*) ***superconducting acceleration and focusing structures*** for efficient injection into ATLAS.

The ISOL Task Force, which met throughout 1999, concluded that an advanced exotic beam facility, now called the Rare Isotope Accelerator (RIA), should utilize a powerful heavy ion driver. The present concept for a CW superconductivity driver is summarized below.

A variety of target concepts developed to handle 100 kW beam powers are illustrated schematically in Figure III-1

B. RADIOISOTOPE PRODUCTION AND HIGH-POWER TARGETRY

(J. Nolen, C. Reed,* I. Gomes,* and A. Hassanein†)

The most critical issues for an advanced ISOL facility concern the generation of radioisotopes in the ISOL production target, and their subsequent extraction as an ion beam. The key technical challenges (target power density, chemical aspects of diffusion, fast effusion geometries, high ionization yields, and ion-source beam emittances) tie into aspects of production mechanisms and target geometry.

The ANL concept for the advanced ISOL facility is based on a high-power superconducting linac providing a broad range of beams, up to uranium. Projected intensities range from close to 10^{16} protons/s to 10^{13} uranium ions/s.

With these intense beams and the high target power densities expected from the Argonne driver linac, target cooling becomes a central issue. In conventional ISOL production schemes the target and ion source are integrally coupled so that cooling the primary target may interfere with the extraction of the radioactive nuclides. With the two-step schemes these functions are physically separated. The ohmic heating by the beam is restricted to the primary target. Advantage is taken of recent developments in cooling with liquid lithium.

*Technology Development Division, ANL; †Energy Technology Division, ANL.

Figure III-2. An operating liquid-lithium pump system circulating 200 gallons/min (100 times the flow needed for the ISOL target) in the Argonne Technology Development Division.

Engineering designs of windowless flowing liquid lithium targets exist at Argonne in the Energy Technology Division and the Technology Development Division, which were developed for stopping 10-MW deuteron beams for the thermonuclear fusion program. Figure III-2 shows a photograph of an operating lithium pump system at Argonne National Laboratory.

C. DEVELOPMENT OF LINAC TECHNOLOGY FOR THE RIA PROJECT

(K. W. Shepard, P. N. Ostroumov, J. Nolen, A. Kolomiets*, M. Kedzie, M. Kelly, M. Portillo, S. Aseev,† and T. Tretyakova*)

The scope of the conceptual design for a driver linac for RIA has been expanded to encompass an unprecedented range of capabilities, including:

- CW beams of the full mass range of ions, from protons through uranium
- Continuously variable output energies up to 400 MeV/nucleon for uranium and higher energies, e.g. 900 MeV protons, for the lighter ions.
- Multiple charge state operation, so that several hundred kilowatts of beam power are available from existing ECR sources for most of the mass range.
- RF beam switching to provide simultaneous CW operation of several targets.

As presently conceived, the linac will provide more than 1.3 GV of accelerating potential, and will consist of an array of more than 400 independently-phased superconducting (SC) cavities of eight different types, ranging in frequency from 58 to 700 MHz. Development of elements of the driver linac is being carried forward at several national laboratories. The technical capabilities developed for the ATLAS SC linac are central in this regard, and are being further developed and extended in several distinct aspects.

Of the eight required cavity geometries, six are low-velocity, low-frequency types of the sort pioneered at ATLAS, and detailed designs for these classes of cavity are being developed with the goal of testing prototypes as soon as feasible. Detailed designs for cryostats, including RF couplers, are also being developed.

The large transverse and longitudinal acceptance available in a SC ion linac opens the possibility of accelerating multiple charge state beams. Such operation can greatly extend the limits of present-day ECR ion source performance, which for the heaviest ions restricts the available beam power in a single-charge-state beam to less than the initial goal of 100 kW, let alone the ultimate goal of 400-kW beams. By operating in a multiple charge state mode, the efficiency of the stripping process is effectively increased by a factor of 3 – 4. This innovation provides directly an increase in the effective beam current and also makes possible the use of multiple strippers, reducing the size of the linac. A further benefit of accelerating multiple charge states is the great reduction in the amount of beam dumped at the stripping points, reducing shielding requirements.

Using numerical simulation techniques, the dynamics of multiple charge state beams are being studied extensively and details of the driver linac lattice, diagnostics, and tuning techniques are being developed. Additionally, experiments are being planned to study several aspects of multiple charge beams that can be tested using the existing ATLAS SC ion linac.

*Institute for Theoretical and Experimental Physics, Moscow, Russia.
†Institute for Nuclear Research, Troitek, Russia.

D. MULTIPLE-CHARGE BEAM DYNAMICS IN AN ION LINAC

(P. N. Ostroumov and K. W. Shepard)

An advanced facility for the production of nuclei far from stability could be based on a high-power driver accelerator providing ion beams over the full mass range from protons to uranium. A beam power of several hundred kilowatts is highly desirable for this application. At present, however, the beam power available for the heavier ions would be limited by ion source capabilities. A simple and cost-effective method to enhance the available beam current would be to accelerate multiple charge states through a superconducting ion linac. The driver linac will consist of two strippers, at ~12 MeV/u and ~85 MeV/u. After the first, the charge state distribution is centered at the charge state q_0=75 for uranium beam. The beam fraction for charge state 75 is 20%; five charges encompass 80% of the incident beam. After the second stripper, 98% of the beam is in four charge states neighboring q_0 = 89, all of which can be accelerated to the end of the linac. The simultaneous acceleration of neighboring charge states becomes possible because the high charge-to-mass ratio makes the required phase offsets small. Figure III-3 shows synchronous phase as a function of charge state calculated for uranium ions at ϕ_{s0} = -30°. This particular example shows that if the linac phase is set for charge state q_0=75, it can accelerate a wide range of charge states. If all charge state are injected at the same time then the bunches of different charge state will oscillate. Therefore one can expect effective emittance growth for multiple charge state beams. The results of numerical simulation of all 5 charge state bunches at the linac portion up to 85.5 MeV/u, just before the second stripper, is shown in Fig. III-4. After the second stripper, the effective longitudinal emittance of the multiple charge state beam is increased by a factor of ~6. We note, however, that this longitudinal emittance is still substantially less than the acceptance of the remaining portion of the SC linac which has been calculated by particle ray tracing and also shown in Fig. III-4.

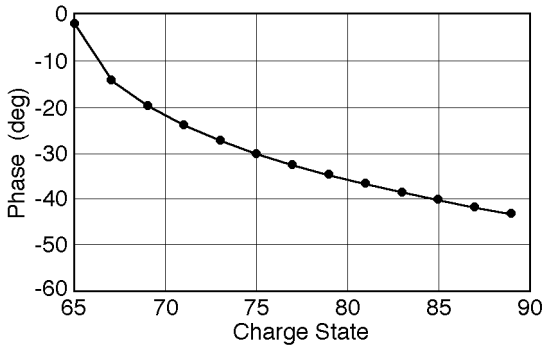

Figure III-3. Synchronous phase as a function of uranium ion charge state. The designed synchronous phase is -30° for q_0 = 75.

Numerical simulations were performed to estimate the effects of various types of errors in accelerator, for both single-charge-state and also for multiple-charge-state beams. In existing SC linacs, phase noise in SRF cavities is generally of the order or less than ±0.3°, and amplitude fluctuations are typically less than ±0.3%. For such systems the effective emittance growth due to multiplicity of charge states in the beam is smaller than the growth due to rf noise. Note that even including both these effects, the total increase in longitudinal emittance is still well below the acceptance of the high energy part of the driver linac.

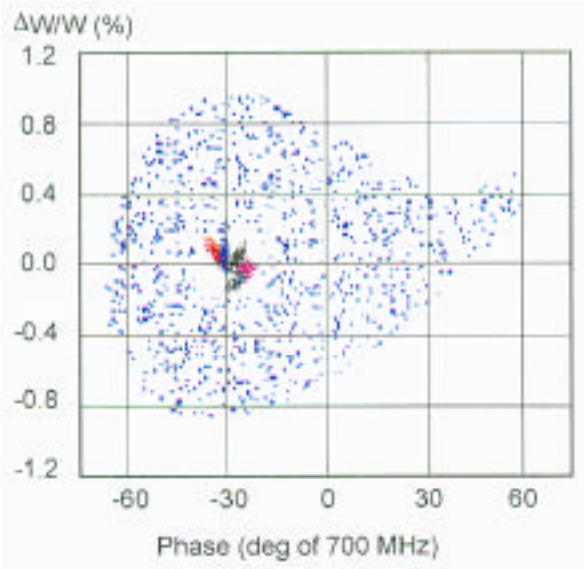

Fig. III-4. Phase space plots of 5 charge state uranium beam at the location of second stripper (85 MeV/u). The large dotted area represents the longitudinal acceptance of the following high-beta linac.

In the ideally tuned linac without any alignment errors the multiplicity of charge states does not produce any emittance growth in transverse phase space. However, in the presence of transverse errors the emittance growth is more severe and less correctable for multiple charge state beams than for single charge state beams. The transverse emittance of multiple charge state beams can grow mostly due to two error effects. The first type of error, mismatch, is caused by errors in tuning or matching the beam into the linac and arises because of errors in measurement of the input beam parameters. The second type of error, a misalignment of the focusing elements, can generally be corrected by using steering magnets to offset any measured deviation of the beam centroid. For a single charge state beam, coherent transverse oscillations and rotation in phase space will not increase effective transverse emittance. In the case of a multiple charge state beam, however, the different charge states have different betatron periods. As the beam proceeds along the linac, the transverse oscillations of the various charge states eventually become uncorrelated and the effective total emittance, summed over all charge states, increases. As we show, the usual corrective steering, can partially correct this situation. Monte Carlo simulations of the dynamics of multiple charge state beams in the presence of alignment errors were performed. A five charge state uranium beam in that portion of the linac between the first and second strippers. Then we tracked the multiple charge state beam through this portion of the linac and noted the increase in transverse emittance resulting from the positioning errors. This entire simulation was then repeated two hundred times, each time with a different, random set of alignment errors. Even for multiple charge state beams, however, emittance growth can be substantially reduced by simple corrective steering procedures. We modeled this by assuming a measurement of beam centroid position and corrective steering to be performed once every four focussing periods. This interval would correspond to the space between cryomodules in the benchmark linac design. The results of our studies show that the transverse emittance growth will not exceed a factor of three for multiple charge state beams in the linac with all types of errors.

In summary, these simulations indicate that it is quite feasible to accelerate 5 charge states of uranium after the first stripper and 4 charge states after the second stripper in this linac.

E. SUPERCONDUCTING CAVITY DEVELOPMENT

e.1. Cavity Production and Testing

(K. W. Shepard, M. P. Kelly, P. Potukuchi,** M. Kedzie, S. Ghosh,** and B. E. Clifft)

Shielding of the test cryostats for ambient magnetic fields has been improved, enabling Q's greater than 10^9 to be observed in, for example, the New Delhi quarter-wave cavities.

RF power available at 350 MHz was upgraded to 400 watts, enabling fields greater than 5 MV/m, as shown in Figure III-5, to be reached in the 350 MHz spoke cavity prototypes for the RIA project. Completion of the testing of these cavities requires high-power pulse conditioning, which awaits the delivery of a 5-kW, 350-MHz amplifier, expected shortly.

Two 97-MHz split-ring cavities were re-built, using off-site vendors for both forming and electron-beam welding procedures. The successful test of these re-built cavities indicate that we established the capability to manufacture these structures through commercial vendors.

*Nuclear Science Centre, New Delhi, India

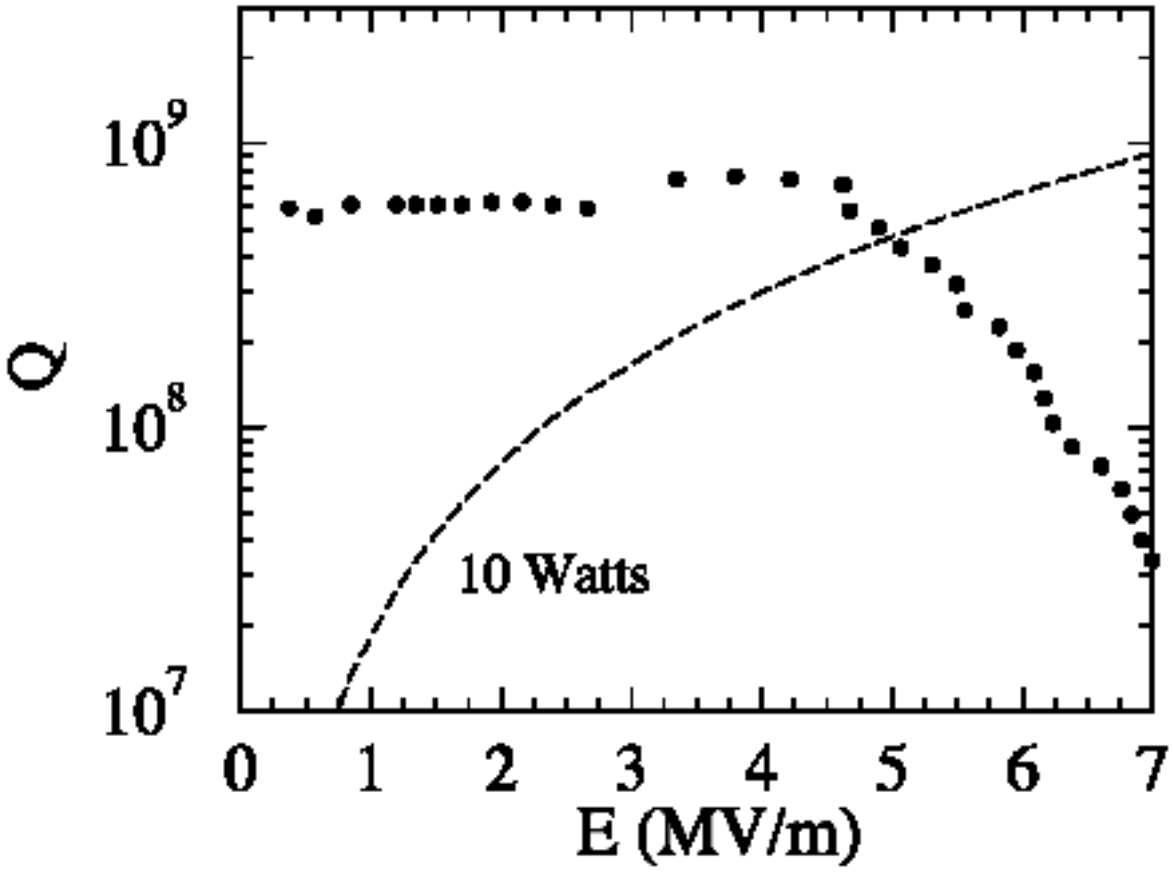

Figure III-5. Measured Q-curve data (filled circles) for 350 MHz spoke cavity. Dashed curve - constant input RF power of 10 W.

e.2. Surface Preparation Laboratory Upgrade (K. W. Shepard, M. Kedzie)

The cavity surface preparation laboratory in Building 203, G150, is being upgraded to, firstly, use vendor-prepared acid mixtures in 55-gallon drum quantities. This upgrade will eliminate most of the hands-on handling of acid required for cavity processing. Secondly, we are adding a capability to perform buffered chemical polishing (BCP) of cavities in addition to the electropolishing procedures that we have used exclusively up to the present. Safety reviews of the additional hardware and procedures are completed, and hardware upgrades are in progress. A high-pressure water-rinser system will also be installed in the near future.

e.3. Superconducting Cavity Design for RIA (K. W. Shepard, T. Tretyakova*)

Six different superconducting drift-tube cavity geometries will be required for the RIA driver, and several more for the secondary accelerator. Initial MAFIA modeling is complete for all six driver cavities, spanning a frequency range from 57 MHz to 350 MHz, and a velocity range from 0.02c to 0.5c. Designs for all six cavities were developed which have satisfactory electromagnetic properties. Mechanical modeling remains to be done before the designs can be finalized.

*Institute for Theoretical and Experimental Physics, Moscow

F. ION SOURCE DEVELOPMENT AT DYNAMITRON

(M. Portillo, J. Nolen, C. Batson, P. Billquist)

A surface ionization source was constructed and tested for use in release studies. The target cup is capable of holding about 15 cm^3 of refractory materials and its centroid lies 3 cm from a primary target which can produce neutrons from $^{9}Be(d,n)$ or $^{11}B(d,n)$ reactions. New refractory materials, such as yttria, were tested as electrical insulators at high temperatures to allow direct contact between the heating filament and the target cup. Also, porous forms of zirconia were used to provide heat shielding for making the target oven as efficient as possible. Target temperatures as high as 1600° were achieved with this scheme at a filament power as low as 200 W. Thus, the power requirements were reduced to almost a factor of 2.5 compared to other heat shielding methods used in the past.

An emittance measurement system was built and used to characterize the ion source. The device is made up of two linear feedthroughs driven by step motors to scan a wire and slit that are 30 cm apart. The slit was 0.5 mm wide and the wire is 0.25 mm in diameter. Figure III-6 shows a plot of the transverse emittance phase space is the x-plane. Simulations using a Monte Carlo model for thermal velocity distributions from a hot surface along with trajectory reconstruction using the code Simion 6.0 agree with the results obtained by measurement.

Figure III-7 shows the resulting analysis applied in order to characterize the phase space area. Integrating the area from the most intense regions to the weakest, the area occupied by the specified current is plotted.

The Dynamitron's performance was tested under high deuteron current conditions. Currents as high as 4.5 μA of the d+ ion were delivered to a ^{9}Be target at the 8°E+25°W beam line at an energy as high as 3.5 MeV. Beam currents of d+ as high as 35 uA have been delivered at 1 MeV, and tests are on-going to deliver such currents at higher energies. Such beams could be used to generate sufficient production rates for measuring time release curves of various refractory materials to survey possible refractory materials for isotope production.

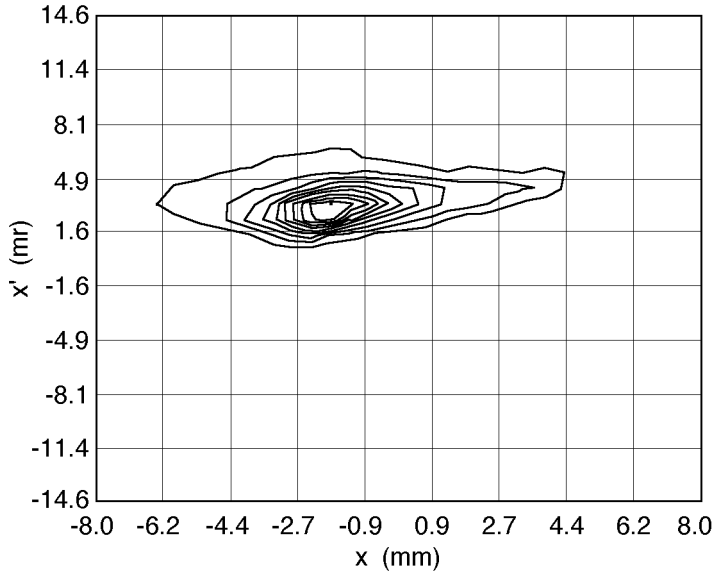

Figure III-6. Transverse phase space emittance plot in the x-plane. The lens after extraction was left off to allow parallel beam to enter the scanning slit.

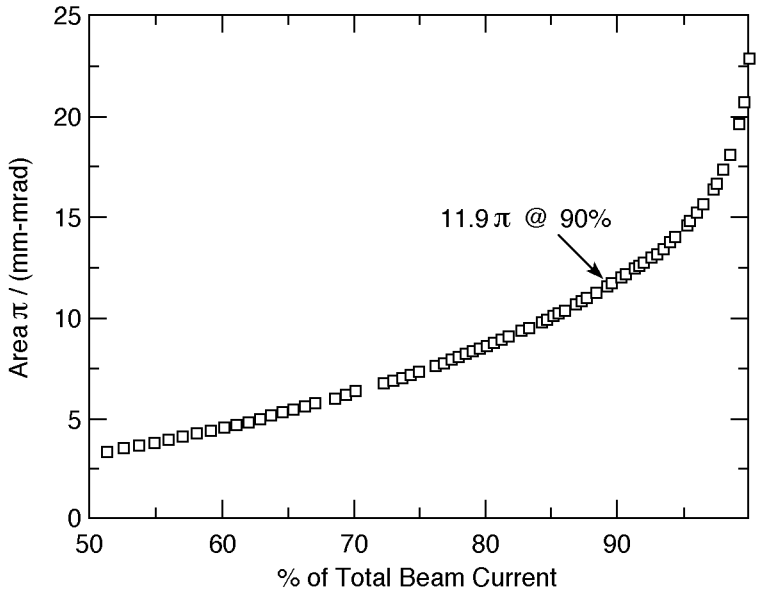

Figure III-7. Phase space area calculated from measurements of the x-plane emittance from a surface ionization source. The area is integrated starting from contour regions of the highest beam intensity. The extraction voltage was 10 kV.

G. THERMAL CONDUCTIVITY MEASUREMENTS OF POROUS MATERIALS AT HIGH TEMPERATURES

(J. A. Nolen, M. Petra and J. Green)

The target materials which are used for ISOL-type radioactive beam facilities are often porous forms of refractory compounds, such as calcium oxide and uranium carbide. At high primary beam power the temperature distribution within such targets depends on the thermal conductivity of these forms of the materials. Very little data exist on the thermal conductivity of such materials at the temperatures of interest, typically 1500 – 2000 ^{o}C, or even higher.

In the present research a simple method based on steady-state electron beam heating was developed to measure the thermal conductivity of porous materials. The emissivity and subsequently the thermal conductivity are evaluated by measuring the temperatures of the hot and cold faces of the specimen (that is T_{hot} and T_{cold} respectively). Three UC_x powder specimens of approximately 1/4 the theoretical density of UC_2 were examined. The total hemispherical emissivity and thermal conductivity were evaluated over a broad temperature range (approximately 850-1750 ^{o}C). The method can be extended to other porous materials that are of interest to ISOL-type facilities.

T_{hot} and T_{cold} were recorded as a function of electron-beam current at an applied voltage equal to 8.7 kV. Calculation of the unknown emissivity of the sample was done by performing an energy balance in the system. The power supplied to the specimen is equal to the power radiated by the cold and hot faces of the sample and the power irradiated by the periphery (Fig. III-8).

The thermal conductivity and emissivity derived from the energy balance in the system were then used as initial input in TAS-TRASYS, a general-purpose thermal modeling code that incorporates a precompiled version of TRASYS. Then, successive iterations in order to match the experimental and computational results yield the final values for the emissivity and thermal conductivity of the specimens (Fig. III-9a-b). An average thermal conductivity (k_{avg}) of those calculated for each specimen was inferred and is plotted as a function of temperature in Fig. III-9a. In Fig. III-9 is also shown the thermal conductivity of theoretical density UC_2 as well as the emissivity of UC for comparison. The simulations assumed that the heating of the lower face of the specimen is uniform and that the specimen is radiating to the environment from the two faces as well as the periphery with a view factor equal to 1. The simulated temperature contour in the specimen calculated with TAS-TRASYS is shown in Fig. III-10a-b for specimen #1. The temperature contour internal to the specimen can be seen in the simulation of one radial brick of the UC_x specimen.

The results for porous UC_x specimens prepared by the ISOLDE prescription is k_{avg} ranging between approximately 0.04 W/cm K and 0.01 W/cm K in the temperature range of approximately 850 ^{o}C and 1750 ^{o}C.

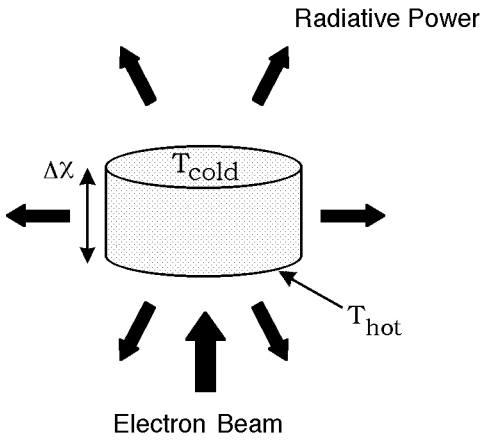

Figure III-8. Enlarged view of the specimen (not to scale). The electron beam heats the lower side of the specimen (of thickness Δx) raising the temperature at T_{hot}. Heat is radiated from the lower and upper sides as well as the periphery of the specimen.

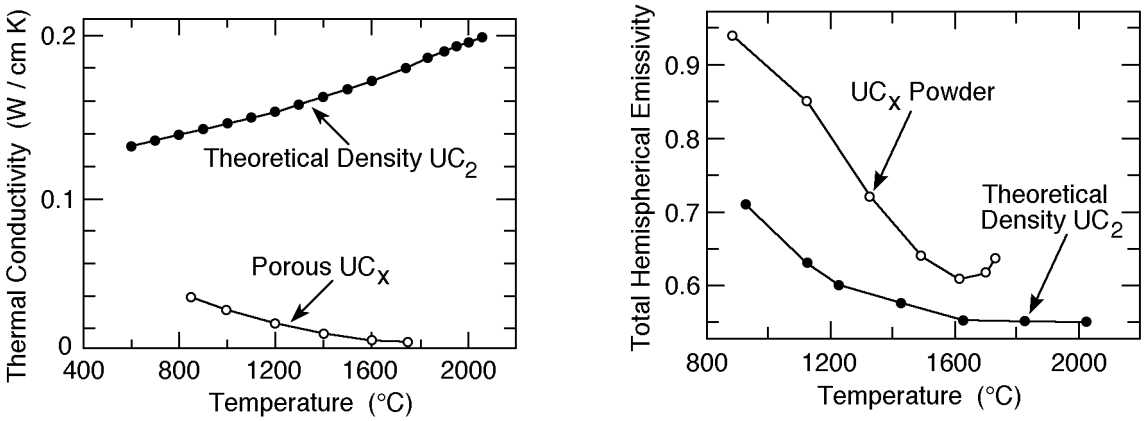

(a) (b)

Figure III-9. a) Variation of the thermal conductivity of theoretical density UC_2 and porous UC_x as a function of temperature. The values shown for the porous UC_x represent average values (that is k_{avg} as a function of T_{avg}). b) Total hemispherical emissivity of theoretical density UC as a function of temperature and UC_x (specimen #1) as a function of T_{avg}.

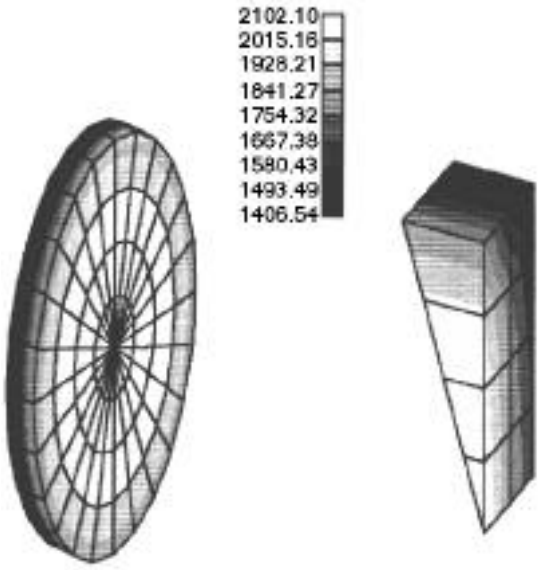

Figure III-10. a) Simulation of the temperature contour in UC_x (specimen #1) performed with TAS-TRASYS. The thermal conductivity and total hemispherical emissivity were assumed equal to 0.0134 W/cm K and 0.634 respectively (Temperatures shown are in ^oC). b) Temperature contour in one 15^o radial brick of the 24 used to simulate the UC_x specimen.

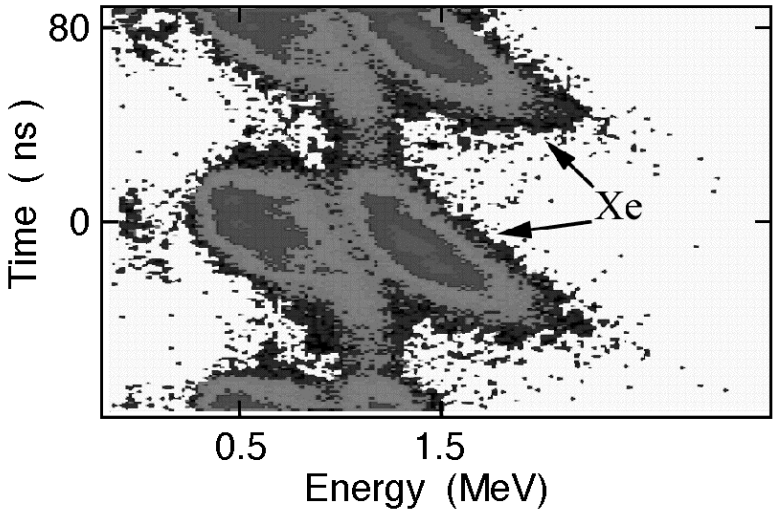

Figure III-11. Measured energy versus time-of-flight spectrum for beam at the RFQ exit for an initially DC beam. Arrows indicate events due to accelerated Xe beam centered at an energy of 1.5 MeV

H. RIB LINAC RFQ BEAM TESTS USING SINGLY-CHARGED A=132 IONS

(P. N. Ostroumov, M. P. Kelly, K. W. Shepard, R. A. Kaye, M. Kedzie, B. E. Clifft)

We performed detailed experimental measurements of singly charged ^{132}Xe beams accelerated through the ANL 12 MHz RFQ for inter-vane voltages up to the design value of 100 keV[1]. As part of an injector to a RIB linac for RIA (Rare Isotope Accelerator) the RFQ would accelerate low energy, low charge-to-mass ratio ion beams with high efficiency (*ie*. CW operation) while simultaneously introducing minimal transverse or longitudinal emittance growth.

We show here some results of a series of measurements using ^{132}Xe beams ranging in energy from 360 to 450 keV injected into the RFQ using the ANL 4 MV Dynamitron. Measured energy versus time-of-flight spectra clearly show events due to accelerated ^{132}Xe ions at the exit of the RFQ. These events are contained in well resolved bunches (~10 ns wide) as measured in a recently constructed silicon detector apparatus placed 30 cm beyond the RFQ exit.

Figure III-11 shows a typical energy versus time-of-flight spectrum for a beam injection energy of 400 keV and an inter-vane voltage of 92 kV. Calibration of the horizontal (energy) axis was performed by direct implantation of 1.3 to 1.7 MeV ^{132}Xe ions into the detector with the RFQ off. The vertical (time) axis contains two complete RF (~80 ns) periods and was measured using standard TOF (time-of-flight) techniques. The two intense regions centered near 1.5 MeV are due to accelerated ^{132}Xe while the events at lower energies are due primarily to detector noise (DC component) and RF pickup. These tests clearly demonstrated the feasibility of CW operation of a room temperature RFQ for low energy, low Z/A ions.

Detailed measurements of emittance and beam transport efficiency using pre-bunched beams, as well as, studies of the long term thermal stability of the RFQ at the highest inter-vane voltages (~100 kV) are underway.

---

[1]Beam Tests of the 12 MHz RFQ RIB Injector for ATLAS, R. A. Kaye, K. W. Shepard, B. E. Clift, M. Kedzie, PAC99 Meeting, March 29-April 2, (1999)